

Quantitative analysis of magnetization reversal in Ni thin films on unpoled and poled (0 1 1) $[\text{PbMg}_{1/3}\text{Nb}_{2/3}\text{O}_3]_{0.68}-[\text{PbTiO}_3]_{0.32}$ piezoelectric substrates

Alexander Tkach^{1,2}, Andreas Kehlberger^{2,3}, Felix Büttner^{2,3,4},
Gerhard Jakob^{2,3}, Stefan Eisebitt^{4,5} and Mathias Kläui^{2,3}

¹ CICECO–Aveiro Institute of Materials, Department of Materials and Ceramic Engineering, University of Aveiro, 3810-193 Aveiro, Portugal

² Institute of Physics, Johannes Gutenberg University Mainz, Staudinger Weg 7, 55128 Mainz, Germany

³ Graduate School of Excellence Materials Science in Mainz, Staudinger Weg 9, 55128 Mainz, Germany

⁴ Institute of Optics and Atomic Physics, Technical University of Berlin, Str. des 17 Juni 135, 10623 Berlin, Germany

⁵ Max-Born-Institut, Max-Born-Str. 2a, 12489 Berlin, Germany

E-mail: atkach@ua.pt

Abstract

The field angle dependence of the magnetization reversal in 20 nm thick polycrystalline Ni films grown on piezoelectric (0 1 1) $[\text{PbMg}_{1/3}\text{Nb}_{2/3}\text{O}_3]_{0.68}-[\text{PbTiO}_3]_{0.32}$ (PMN–PT) substrates is analysed quantitatively to study the magnetic anisotropy induced in the film by poling the piezosubstrate. While the PMN–PT is in the unpoled state, the magnetization reversal is almost isotropic as expected from the polycrystalline nature of the film and corresponding to an orientation ratio (OR) of 1.2. The orientation ratio is obtained by fitting the angular dependence of normalized remanent magnetization to an adapted Stoner–Wohlfarth relation. Upon poling the piezosubstrate, a strong uniaxial anisotropy, whose hard axis is oriented along the [1 0 0] direction of the PMN–PT, is induced, yielding an OR of 3.1. The angular dependence of the coercivity for the poled state is found to consist of a strong increase for increasing field angles away from the easy axis direction and of a sharp decrease for angles close to the hard direction. It is best described by a two-phase model, implying that the magnetization reversal is determined by both, coherent rotation of the magnetic moments, according to the Stoner–Wohlfarth model, and the gradual displacement of the domain walls in obedience to the Kondorsky model.

Keywords: electric-field control of magnetism, magnetic anisotropy, multiferroic heterostructure, ferroelectrics, magnetic materials

1. Introduction

Electric-field (E) control of magnetization (M) has a number of advantages over current-driven control because of its possibly

reduced energy consumption [1, 2]. For several decades, the capability of achieving this type of control has been tested in a special class of materials, so-called magnetoelectrics (MEs) or multiferroics, in which M (or the electric polarization P) is

expected to be modulated by E (or the magnetic field H) [1]. For potential applications in novel multifunctional devices, such as low-power spintronic devices, magnetic recording media, magnetic sensors, and microwave devices, the magnetoelectric coupling should be strong at room temperature, a feature which is difficult to obtain in single phase multiferroics [2]. However, artificial multiferroics, which consist of room-temperature ferromagnetic and ferroelectric materials and in which ferroic properties are collected from these different phases, have revealed promising results to provide broader benefits to the future development of the aforementioned applications [1, 2]. Artificial multiferroics can be multiferroic composites, usually consisting of ferroelectric and ferromagnetic grains, or multiferroic heterostructures, consisting of ferroelectric and ferromagnetic layers [2].

Particularly, much attention has been paid to strain-mediated magnetoelectric coupling between room-temperature ferromagnetic 3d metal Ni films and $[\text{PbMg}_{1/3}\text{Nb}_{2/3}\text{O}_3]_{1-x}[\text{PbTiO}_3]_x$ (PMN-PT) ferroelectric substrates [3–9]. In such a structure, upon application of an electric field, the piezoactive PMN-PT substrate induces a strain in the Ni film, and hence modifies its magnetic properties due to the inverse magnetostrictive effect. It was shown that the maximum difference in the magnetic and magnetotransport response of a Ni film occurs between the poled state of a (011)-oriented PMN-PT substrate and the unpoled one [3, 8]. Moreover, a state close to the unpoled one can be reached again by application of an electric field pulse with amplitude close to the coercive electric field value, but opposite sign regarding the poling field. Thus, a hysteretic dependence of the magnetic and magnetotransport responses on electric field can be obtained by using accurate polarization control [8]. However, while a number of reports of the effects measured along certain directions have been published, a full quantitative analysis is still lacking. To perform such an analysis and thus to understand the effect, one does need to obtain a full angular dependence as only this quantifies the resulting anisotropies. Hence since in this hysteretic behaviour the poled and unpoled states are the two states that need to be compared, in this work, we focus on a quantitative analysis of magnetic anisotropy manipulation and magnetization switching in Ni/PMN-PT multiferroic heterostructures between these two non-volatile states, using magneto-optic Kerr effect (MOKE) magnetometry.

2. Experimental procedure

The samples were prepared on polished (011)-oriented $[\text{PbMg}_{1/3}\text{Nb}_{2/3}\text{O}_3]_{1-x}[\text{PbTiO}_3]_x$ ($x = 0.32$) substrates (Atom Optics Co., LTD, Shanghai, China) of $5 \times 5 \times 0.5 \text{ mm}^3$ size, which were annealed at $300 \text{ }^\circ\text{C}$ for 30 min. First, top (10 nm) and bottom (50 nm) Pt layers were DC-magnetron sputtered on both sides of the PMN-PT substrate using 5 nm thick adhesion layers of Cr. Then, polycrystalline Ni films with a thickness of 20 nm were deposited on the top side by DC-magnetron sputtering using an Ar pressure of 10^{-2} mbar.

A voltage supply (FuG MCN 35-200) was used for application of the electric fields up to 4 kV cm^{-1} between the top

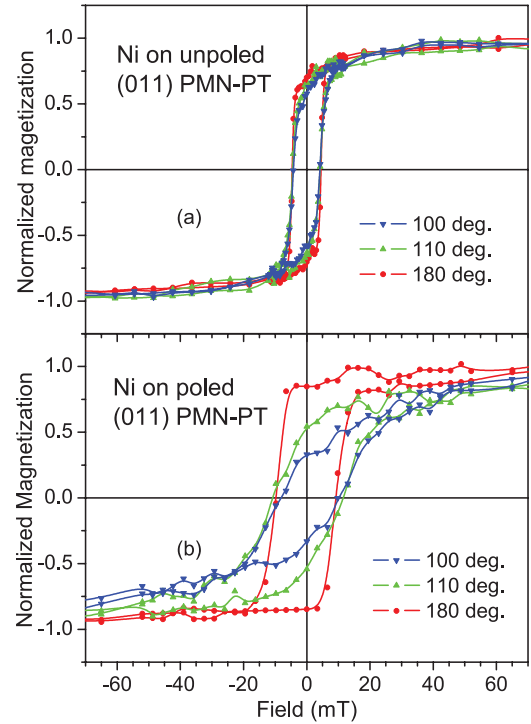


Figure 1. Room-temperature magnetization hysteresis loops of the polycrystalline Ni films on unpoled (a) and poled (011) PMN-PT (b) for an applied field orientation of 100° , 110° and 180° away from the $[01\bar{1}]$ (y) direction of the PMN-PT.

(Ni film) and bottom (Pt) electrodes of PMN-PT. An electromagnet (GMW 3470) powered by a bipolar power supply (Kepco BOP 36-6M), generating the magnetic field up to 0.3 T, was used for room-temperature MOKE measurements together with a sample rotator. A linearly polarized beam was produced by a HeNe laser system (CVI Melles Griot) with a wavelength of $\lambda = 632.8 \text{ nm}$ and an output power of 5 mW, passing through a Glan-Thompson polarizer (Thorlabs) with an extinction coefficient of 10^{-5} . The beam reflected from the sample was periodically modulated at 50 kHz between left and right circularly polarized light by a photoelastic modulator (Hinds Instruments PEM-100), transmitted through an analyser (polarizer with the transmission axis rotated by 45 degrees) and finally detected by a photosensitive fast responding diode (Hinds Instruments DET-200), connected to a lock-in amplifier (Signal Recovery 7225 DSP) with the modulation signal used as a reference input.

3. Results and discussion

Ferromagnetic hysteresis loops obtained by superconducting quantum interference device magnetometry on such Ni/PMN-PT heterostructures along the $[100]$ (x) and $[01\bar{1}]$ (y) directions of PMN-PT were recently reported, revealing a saturation magnetization of $255 \pm 15 \text{ kA m}^{-1}$ at room temperature [8]. Poling of the PMN-PT substrate was found to induce a strong magnetic anisotropy in the Ni film where the x direction is a hard axis (HA) and y is an easy axis (EA) [3, 4, 8]. In order to achieve a more detailed characterization of the angular dependence of magnetization

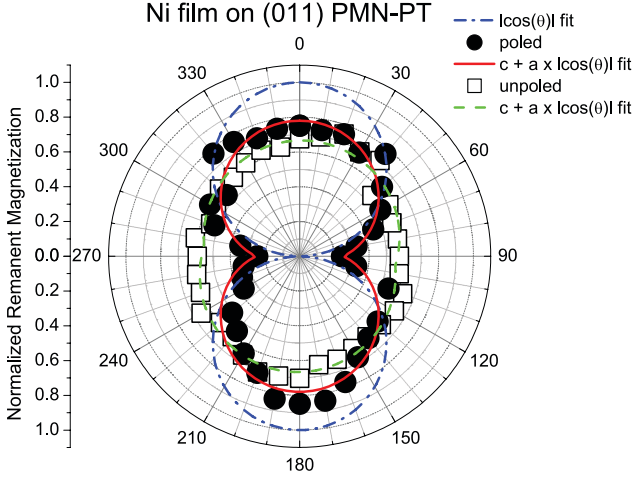


Figure 2. Angular dependence of the normalized remanent magnetization M_r/M_s , deduced from MOKE magnetization loops of the Ni films on (0 1 1) PMN-PT in the unpoled (open squares) and poled states (solid circles). The dash-dot line is the Stoner-Wohlfarth $|\cos(\theta)|$ fit, while the dashed and solid lines represent the least-square fits of the M_r/M_s data measured in unpoled and poled states, respectively, using equation (2). The error bars are smaller than the symbol sizes.

reversal properties in Ni/PMN-PT heterostructure, we have measured hysteresis loops at different in-plane field directions with intervals of 10° by MOKE technique. Figure 1 shows several room-temperature magnetization hysteresis loops of the polycrystalline Ni film on the unpoled (figure 1(a)) and the poled (1 1 0) PMN-PT (figure 1(b)) for different applied field angles with respect to the $[0 1 \bar{1}]$ (y) direction of the PMN-PT. In each case, the magnetization is normalized to a reference signal (magnetization M_s), which is the magnetization signal at the maximum applied field of $H = 120$ mT for the unpoled PMN-PT and 156 mT for the poled one. These field values are in saturation, i.e. beyond the corresponding saturation fields that is found to increase from ~ 54 mT to ~ 132 mT upon poling, where the latter then corresponds to the hard axis anisotropy field H_a (see figure 1(b)) [8].

Before poling, all the loops show a very similar behaviour with a normalized remanent magnetization of 0.65 ± 0.10 and a coercive field of 4.2 ± 0.4 mT (see figure 1(a)). In contrast to the absence of significant magnetic anisotropy in the unpoled Ni/PMN-PT heterostructure, we could clearly observe an induced anisotropy after poling. As seen from figure 1(b), the normalized remanent magnetization continuously decreases from 0.85 to 0.33 with a rotation from y direction toward x direction. However, as figure 1(b) also shows, the coercive field varies non-monotonously for such a rotation, revealing a maximum around 110° .

As an overview the angular dependences of the core reversal quantities extracted from the hysteresis loops measured from 0° to 360° are plotted in figures 2 and 3. Figure 2 shows the normalized remanent magnetization M_r/M_s , whereas figure 3 presents the coercive field H_c . In agreement with the loops shown in figure 1, a much more pronounced angular dependence of M_r/M_s with a periodicity of 180° (which is the signature of uniaxial anisotropy) is observed for the poled sample. Moreover, the shape of the angular dependence of M_r/M_s for

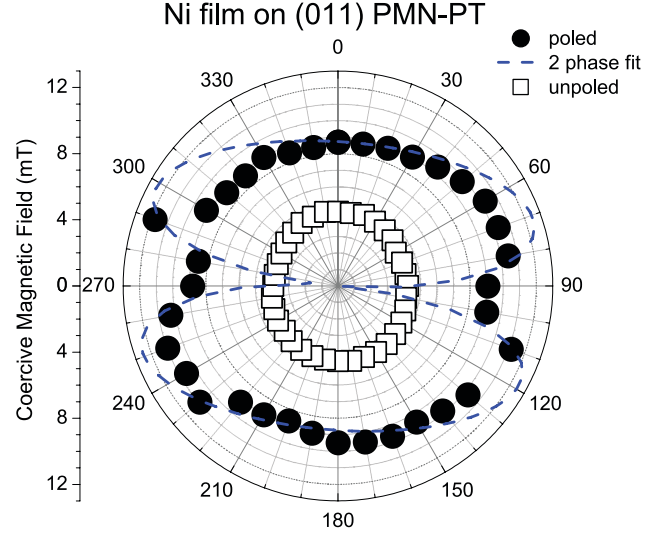


Figure 3. Angular dependence of the coercive magnetic field H_c , deduced from MOKE magnetization loops of the Ni films on (0 1 1) PMN-PT in unpoled (open squares) and poled states (solid circles). The dashed line is the least-square fit of the H_c data measured in poled state, using equation (4). The error bars are smaller than the symbol sizes.

the Ni film on the poled PMN-PT is similar to a theoretically predicted $|\cos(\theta)|$ relation (dash-dot line in figure 2) that presents the ideal case of the Stoner-Wohlfarth (SW) model [10]. This model is suitable for single domain magnets with a uniaxial magnetic anisotropy, in which the normalized remanent magnetization is exactly 1 along the easy axis (0° and 180°) and decreases coherently towards the hard axis (90° and 270°), where M_r/M_s vanishes. However, the M_r/M_s values measured in our Ni film on poled (0 1 1) PMN-PT do not reach 1 and do not vanish completely showing that there is no perfect coherent rotation reversal. This deviation is expected for continuous films and caused by the fact that the Ni film is polycrystalline and the anisotropy axes of different grains are not aligned. Moreover, because the probed area is much larger than the critical size of single domain, incoherent rotation and multi-domain states take place in the film, thus being an additional source of the anisotropy dispersion.

To quantify the partial or imperfect uniaxial magnetic anisotropy one can obtain an orientation ratio conventionally defined as:

$$OR = M_{\text{rea}}/M_{\text{rha}}, \quad (1)$$

where M_{rea} and M_{rha} are the remanent magnetization values measured along the EA and the HA, respectively [11]. However, for a more robust analysis, instead of the conventional equation (1), based only on the two-point measurement (M_{rea} and M_{rha}), one can consider M_r/M_s data in the entire field orientation range (θ) by using an adapted SW relation [12]:

$$M_r/M_s(\theta) = c + a|\cos(\theta)|. \quad (2)$$

Hereby, from the fit parameters c and a , defining the degree of uniaxial alignment, one can calculate the extrapolated magnetic orientation ratio [12]:

$$OR' = M'_{\text{rea}}/M'_{\text{rha}} = (a + c)/c. \quad (3)$$

Thus, performing the least-square fit of the experimental M_r/M_s data for the Ni film on poled (0 1 1) PMN–PT to equation (2), as shown in figure 2 by a solid line, c and a parameters of 0.25 and 0.53, respectively, were obtained. Then according to equation (3), the value of the extrapolated orientation ratio OR' is 3.1, while the conventional OR obtained using equation (1) is 3.5. The difference between the OR and OR' is within 12% and hence the conventional OR can also be used for estimation of this system. However, the extrapolated OR' , being based not only on two specific values but on the entire field orientation dependence of the remanent magnetization, is a refined value that is more robust against measurement uncertainties or small angle range anomalies [12]. On the other hand, the OR and OR' values for Ni film on (0 1 1) PMN–PT in the unpoled state (see dashed line in figure 2) were found to be close to 1 (1.3 and 1.2, respectively), confirming its nearly isotropic in-plane magnetic behaviour. Small deviation from unity and hence magnetic anisotropy in the unpoled state can be induced for instance by stray magnetic fields from the oblique angle magnetron sputtering during the film deposition [9].

The observation of the variations in the angular dependence of M_r/M_s and H_c of the Ni films in the unpoled and poled states of the PMN–PT substrates is related to the strain response of the (0 1 1) $[PbMg_{1/3}Nb_{2/3}O_3]_{0.68}-[PbTiO_3]_{0.32}$ single crystal. According to Kim *et al* [6], when PMN–PT is in the unpoled state, Ni in the magnetoelectric Ni/PMN–PT structure is subjected to negligible strain ($\varepsilon_x = \varepsilon_y = 0$). Moreover, although strain is produced upon poling the PMN–PT substrate, it is compressive along both x and y axes. So only the strain difference between these two orientations should lead to variation in the magnetic anisotropy of polycrystalline Ni films right at the poling electric field of $\sim 2.5 \text{ kV cm}^{-1}$. However, after removal of the electric field, very different remanent compressive strains along the different directions of $\varepsilon_x = -300 \text{ ppm}$ and $\varepsilon_y = -1000 \text{ ppm}$ are produced by PMN–PT in the poled state due to the different signs of d_{31} and d_{32} piezocoefficients [6], inducing large magnetic anisotropy in the Ni film. Since Ni has a negative magnetostrictive coefficient [13], induced magnetoelastic anisotropy causes its magnetic dipoles to align along the dominant compressive strain direction, i.e. y axis, which thus corresponds to the EA induced for the poled state [4, 8]. Additionally, one has to take into account that the OR is proportional to the magnetic anisotropy [11], which is caused by the stress difference in the film in the x and y axis directions. Thus, one should expect the variation in the orientation ratio of Ni films on (0 1 1) PMN–PT substrates upon poling. In complete agreement with this analysis, the OR' value in our Ni films varies from 1.2 to 3.1 that is compatible with an increase of the anisotropy constant to $\sim 17 \text{ kJ m}^{-3}$ upon poling [8].

Now we turn to the angular dependence of H_c for Ni/PMN–PT heterostructures, presented in figure 3, and consider it in relation to the magnetization reversal mechanism. As mentioned above, the SW model is one of the most important models for a magnetization reversal mechanism that is based on coherent rotation of all spins [10]. According to this model, H_c decreases monotonously with increasing angle between the EA and applied magnetic field θ . Another important magnetization reversal mechanism is the Kondorsky model applied

to the uniaxial magnets, where the magnetization reversal is controlled by domain wall (DW) depinning [14]. According to this model, H_c increases monotonously with increasing θ . However, as it was shown in figure 1 and depicted in figure 3 in detail, the angular dependence of H_c for a Ni film on poled PMN–PT is not a monotonous function for the rotation from the easy to the hard axis and hence cannot be explained by any of these models alone. However, such a non-monotonous dependence has been already observed for (Sm,Zr)(Co,Cu,Fe) alloys [14], epitaxial (100) and (110) $La_{0.67}Sr_{0.33}MnO_3$ films [15, 16], strip-patterned FeTa films [17], amorphous $Co_{40}Fe_{40}B_{20}$ films on $YMnO_3$ substrates [18] and FeCo films on (0 1 1) PMN/PT substrates [19]. Thus, a two-phase model, which as a concept was first introduced by Néel [20], was proposed to fit the angular dependence of H_c as follows:

$$H_c^{2-ph}(\theta) = H_c(0)(N_x + N_N)\cos\theta/[N_y\sin^2\theta + (N_x + N_N)\cos^2\theta], \quad (4)$$

where $H_c(0)$ is the nucleation field of domain walls, whereas N_x and N_y are the demagnetizing factors along the x axis direction and y axis direction (easy axis), respectively [14]. Both axes are in the plane of the magnetic field and of the magnetization rotation. $N_N = H_a/M_s$ is a formal parameter that can be interpreted as an effective demagnetizing factor due to the effect of an anisotropy other than the shape anisotropy, where H_a and M_s are the anisotropy field and saturation magnetization, respectively. Thus, this model contains both DW motion, dominant at angles below θ_{max} , and the large rotation of the magnetization in the domains for angles close to the hard direction. For a large ratio $n = (N_x + N_N)/N_y$, implying a strong anisotropy as compared to shape anisotropy, the above equation reduces to the original Kondorsky relation.

Indeed, our experimental results, consisting of the initial increase for a rotation away from the EA and the rapid decrease approaching HA, can be fitted using equation (4) (dashed line in figure 3) with fitting parameters $n = (N_x + N_N)/N_y = 9.4$ and $H_c(0) = 7.7 \text{ mT}$. However, the measured hard axis minimum is finite instead of $H_c^{2-ph}(90^\circ) = 0$ deduced from the two-phase model. Although the finite minimum may be due to a slight misalignment from the hard axis direction, it could also be an indication of some spread in the easy axis directions. Such an easy axis distribution, resulting in $H_c^{2-ph}(90^\circ) \neq 0$, is expected for polycrystalline materials [14], which is the case of our Ni films. Moreover, the spread in the easy axis directions can be not only due to that the anisotropy axes of different grains are not fully aligned but also due to a presence of ferroelectric domains in the piezo-substrate and their influence on the (mis)orientation of the magnetic domains in Ni film via magnetoelectric coupling [21]. This is supported by the angular dependence of the M_r/M_s ratio, showing a finite minimum in the hard axis direction as well (see figure 2). Thus, although not perfect, the two-phase model can be applied to the angular dependence of H_c for the Ni films after poling the PMN–PT substrate. Hence such a variation can be ascribed to a combination of Kondorsky-type reversal and coherent rotation-type reversal switching mechanisms occurring simultaneously.

On the other hand, in unpoled state H_c shows no significant variation with rotation angle, in accordance with a nearly isotropic magnetic response reflected by OR of 1.2 only. At the same time, the coercivity variation between the unpoled and poled states of PMN–PT is from 100 to 200% depending on the field direction, implying that the energy barrier to magnetization reversal is significantly changed by clamping the magnetic domains so that a higher magnetic field is needed for their reorientation. It was previously reported [22] that uniaxial compressive strain increases the coercivity of Ni and due to the difference in the remanent strain along x and y directions we have a uniaxial strain component in our Ni films as well.

Furthermore, operating in the vicinity of the coercive electric field of PMN–PT that is close to the poling field (but with the opposite sign), it is possible to take advantage of the non-180° polarization rotation and obtain a state close to the unpoled one [4, 8]. Thus, two reversible and permanent strain states, having potential in memory device applications [1] and quantitatively analysed in this work, can be produced, causing the in-plane uniaxial anisotropy reorientation of Ni/PMN–PT heterostructures through the converse ME effect.

4. Conclusions

In conclusion, we have demonstrated and quantified the large non-volatile effect of the poling of (0 1 1) PMN–PT piezosubstrates on the magnetic anisotropy of Ni films at room temperature. The induced anisotropic in-plane strain gives rise to a strong uniaxial magnetic in-plane anisotropy. Both the coercive field and the M_r/M_s ratio become strongly dependent on the magnetic field direction, showing a pronounced minimum along x , which is thus a hard axis. The angular dependence of the normalized remanent magnetization is well fitted to the SW relation adapted for polycrystalline films, revealing a significant increase in OR' from 1.2 to 3.1 upon poling the PMN–PT substrate. At the same time, the two-phase model gives a good quantitative agreement with the experimentally measured angular dependence of the coercivity, showing non-monotonous variation of H_c between the easy and hard axis directions. On the other hand, it is clear that the anisotropy is not perfectly uniform, since there are deviations of the experimental data from the uniaxial anisotropy model. Such deviations, indicating that there are variations in the magnetic properties across the probed area, are explained by polycrystallinity of the Ni films, their multi-domain states and misorientation of the magnetic domains in Ni film via magnetoelectric coupling with the ferroelectric domains in PMN–PT substrate.

Acknowledgments

This work was funded by the EU's 7th Framework Program IFOX (NMP3-LA-2010 246102), the Graduate School of Excellence Materials Science in Mainz (GSC 266 MAINZ), the German Science Foundation (DFG KL1811, SFB TRR173 Spin+X) and the ERC (2007-Stg 208162, 2014-PoC 665672). A. Tkach acknowledges also funding within the scope of the project CICECO-Aveiro Institute of Materials POCI-01-0145-FEDER-007679 (FCT Ref. UID/CTM/50011/2013), financed by national funds through the FCT/MEC and when appropriate co-financed by FEDER under the PT2020 Partnership Agreement as well as within independent researcher grant IF/00602/2013.

References

- [1] Ma J, Hu J, Li Z and Na C-W 2011 *Adv. Mater.* **23** 1062
- [2] Hu J-M, Chen L-Q and Nan C-W 2016 *Adv. Mater.* **28** 15
- [3] Wu T, Bur A, Zhao P, Mohanchandra K P, Wong K, Wang K L, Lynch C S and Carman G P 2011 *Appl. Phys. Lett.* **98** 012504
- [4] Wu T, Bur A, Wong K, Hockel J L, Hsu C-J, Kim H K D, Wang K L and Carman G P 2011 *J. Appl. Phys.* **109** 07D732
- [5] Hockel J L, Bur A, Wu T, Wetzlar K P and Carman G P 2012 *Appl. Phys. Lett.* **100** 022401
- [6] Kim H K D, Schelhas L T, Keller S, Hockel J L, Tolbert S H and Carman G P 2013 *Nano Lett.* **13** 884
- [7] Finizio S *et al* 2014 *Phys. Rev. Appl.* **1** 021001
- [8] Tkach A, Kehlberger A, Büttner F, Jakob G, Eisebitt S and Kläui M 2015 *Appl. Phys. Lett.* **106** 062404
- [9] Hong B *et al* 2016 *Mater. Lett.* **169** 110
- [10] Stoner E C and Wohlfarth E P 1948 *Philos. Trans. R. Soc. A* **240** 599
- [11] Yu M, Choe G and Johnson K E 2002 *J. Appl. Phys.* **91** 7071
- [12] Idigoras O, Suszka A K, Vavassori P, Obry B, Hillebrands B, Landeros P and Berger A 2014 *J. Appl. Phys.* **115** 083912
- [13] Berger L 1965 *Phys. Rev.* **138** A1083
- [14] Suponev N P, Grechishkin R M, Lyakhova M B and Pushkar Yu E 1996 *J. Magn. Magn. Mater.* **157/158** 376
- [15] Mathews M, Houwman E P, Boschker H, Rijnders G and Blank D H A 2010 *J. Appl. Phys.* **107** 013904
- [16] Boschker H, Kautz J, Houwman E P, Koster G, Blank D H A and Rijnders G 2010 *J. Appl. Phys.* **108** 103906
- [17] Han X M, Ma J H, Wang Z, Yao Y L, Zuo Y L, Xi L and Xue D S 2013 *J. Phys. D: Appl. Phys.* **46** 485004
- [18] Wang J W *et al* 2013 *Appl. Phys. Lett.* **102** 102906
- [19] Yang C, Wang F, Zhang C, Zhou C and Jiang C 2015 *J. Phys. D: Appl. Phys.* **48** 435001
- [20] Neel L, Pauthenet R, Rimet G and Giron V S 1960 *J. Appl. Phys.* **31** S27
- [21] Fusil S, Garcia V, Barthelemy A and Bibes M 2014 *Annu. Rev. Mater. Res.* **44** 91
- [22] Wu T, Bur A, Hockel J L, Wong K, Chung T-K and Carman G P 2011 *IEEE Magn. Lett.* **2** 6000104